
Article:
Russell, C orcid.org/0000-0002-7322-8255, Swithenbank, M orcid.org/0000-0002-6146-1818, Wood, CD orcid.org/0000-0003-1679-5410 et al. (5 more authors) (2016) Integrated On-Chip THz Sensors for Fluidic Systems Fabricated Using Flexible Polyimide Films. IEEE Transactions on Terahertz Science & Technology, 6 (4). pp. 619-624. ISSN 2156-342X

https://doi.org/10.1109/TTHZ.2016.2557724

Integrated on-chip THz sensors for fluidic systems fabricated using flexible polyimide films

Christopher Russell, Matthew Swithenbank, Christopher D. Wood, Andrew D. Burnett, Lianhe Li, Edmund H. Linfield, A. Giles Davies and John E. Cunningham

***Abstract*—We investigate the use of an on-chip terahertz (THz) frequency sensor formed on a flexible, thin-film polyimide substrate to measure the properties of liquids encapsulated in a glass-walled capillary. We observe changes in the attenuation and velocity of the time-domain THz signal, which allows extraction of the broadband THz refractive index and relative attenuation coefficients of the liquid. The technique is used for sensing members of a homologous series of primary alcohols, and the results compared with those obtained from a free-space THz-TDS system.**

***Index Terms*—Fluidics, planar Goubau lines, on-chip sensing, low-temperature-grown GaAs, terahertz.**

I. Introduction

TERAHERTZ frequency time-domain spectroscopy (THz-TDS) is a potentially powerful tool for chemists and biologists to investigate the dynamics and function of hydrated biological systems [1]. However, such measurements are often limited by the strong absorption of liquid water in this frequency range.

Free-space THz measurements typically employ a transmission geometry, using a suitably thin sample cell to minimise attenuation [2]. However, the closely-spaced material interfaces of the cell introduce etalons into the measured time-domain signal, arising from interfacial reflections, which can adversely affect subsequent data analysis. Alternatively, reflection measurements, such as those used in THz-attenuated total reflection spectroscopy [3] can be employed to measure thicker liquid samples [4], but here the majority of the reflected signal interacts only with the sample surface, which is not necessarily representative of the bulk. Additionally, free-space THz systems are often diffraction limited and, owing to reflections in the emitter/detector crystals, typically provide only a coarse frequency-resolution (10s of GHz) [5]. To overcome these limitations, lithographically-defined on-chip systems can be used, but these characteristically have a reduced bandwidth compared with free-space systems, owing to strong signal attenuation and dispersion [6].

To date, the on-chip systems that have been used for the study of bulk fluid samples in the THz regime use either microstrip line (MSL) [7] or planar Goubau line (PGL) [8, 9] geometries, whilst coplanar waveguides (CPWs) have been used at lower frequencies (1 – 5 GHz) [10]. In each of these systems, the evanescent electric field propagating along the waveguide can be employed for the analysis of overlaid dielectric materials, by observing changes induced by proximal samples in the transmission of pulses over the length of the waveguide, such as the attenuation or the propagation velocity. Typically, such waveguides are fabricated on crystalline substrates including quartz [6, 11], sapphire [12] and GaAs [12], *inter alia*. The bandwidth of these devices is then often enhanced by mechanical lapping of the substrate material [6], or, more recently by using polymer substrates such as Tsurupica [11] and polyimide [13], which are available as thin films (10s of microns thick). These allow both improved bandwidth and sensitivity whilst also offering the additional benefits of reduced cost and increased durability. Overall, however, the PGL is the preferred choice of waveguide for spectroscopic measurements, owing to the increased extent of evanescent field which it shows when compared with other geometries.

A number of materials have been used to define a fluidic channel for integration with on-chip THz-TDS systems including THz-transparent, high-resistivity silicon [9, 14] and polydimethylsiloxane (PDMS), which allow inclusion of integrated microfluidic components such as filters and mixers [15]. However, the choice of both substrate and fluidic-channel material can impose limitations on which liquids can be measured. Effects detrimental to the device's performance must be considered, such as delamination of the fluidic channel

This work was supported by funding from the EPSRC (**UK**), the ERC program 'TOSCA', the DTRA (US) (HDTRA1 -14-C-0013), the Royal Society and the Wolfson Foundation.

C. Russell, M. Swithenbank, C. D. Wood, A. D. Burnett, L. Li, E. H. Linfield A. G. Davies and J. E. Cunningham are with the School of Electronic and Electrical Engineering, University of Leeds, Leeds LS2 9JT, UK (email c.russell@leeds.ac.uk).

A. D. Burnett is also with the School of Chemistry, University of Leeds, Leeds LS2 9JT, UK.

The data associated with this paper are openly available from the University of Leeds repository. http://doi.org/10.5518/18

from the substrate, or etching of the surrounding materials [16].

In this article, we report the development of THz TD transmission line devices on the top surface of a 13-µm-thick polyimide film [13]. The flexibility of this substrate allows the transmission line to be wrapped around a thin-walled capillary, with the transmission line patterned outwards. This allows for an uninterrupted optical path to the photoconductive switches (PCSs), and on-chip THz measurements to be performed on liquids enclosed within the capillary. The choice of liquid in our system is thus limited only by its chemical interaction with the capillary material, which can then be chosen to suit different applications.

II. Design Concept

We have developed a reflection-mode PGL geometry which allows both the generated and transmitted signals, produced and detected using PCSs, to be recorded within a single THz-TD measurement (see Fig. 1(b) and section III) [11]. The generated THz signal propagates along the PGL, which is wrapped around a fluid filled capillary, and is reflected back to the detector from an open-circuit termination. The resulting time-domain signal includes both the input and reflected pulses, allowing the simultaneous acquisition of the generated signal and a comparative measurement from the sample. Signal reflections arising from the electrical interconnects of the bias arms used to define the low-temperature-grown GaAs (LT-GaAs) based PCS, and from the grounded connection of the PGL, were removed from the time window of the measurements by ensuring that they had sufficiently long electrical lengths; these extended sections of the transmission line are referred to as 'parasitic regions' forthwith. Since the probing signal has propagated twice through the overlaid liquid, the interaction length between the THz signal and the liquid sample in this arrangement is twice the distance between the PCSs and the end of the transmission line. By confining the liquid under test to a capillary around which the device is wrapped, we avoided introducing interfacial boundaries arising from the fluidic channel geometry. This eliminated etalons, whilst maximising the signal-sample interaction length, and so correspondingly increased the device sensitivity. We note that this approach would not have been possible with either MSL or grounded-CPW device geometries, in which the rear surface of the substrate must necessarily be metallised to form a back-plane.

The polyimide substrate was bonded to the outside of a capillary, which had sufficiently thin walls (10 µm) to allow the liquid inside to be interrogated by the THz evanescent field. The outer diameter of the capillary (3 mm) was chosen to be sufficiently large to prevent the ends of the transmission line from overlapping, and to prevent any unwanted attenuation, reflections, or cross-coupling between ends of the PGL which can occur if electrical separation of conductors, less than 100 µm are used [17].

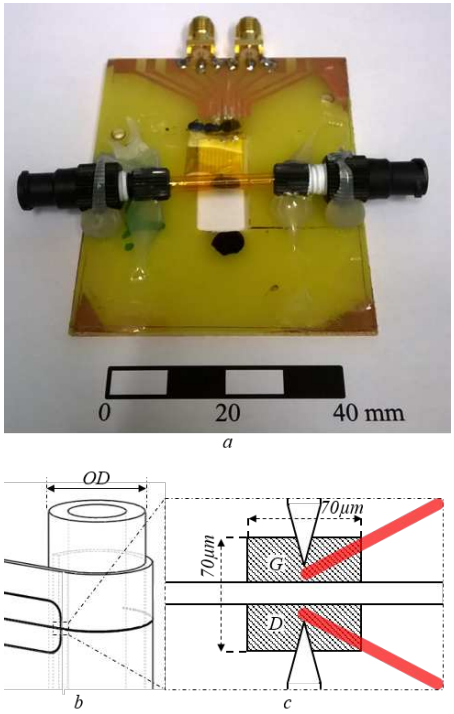

Fig. 1. (a) Photograph of the PGL on polyimide, wrapped around a quartz capillary, itself capped with Luer connectors. The system is mounted on printed circuit board, with attached SMA connectors used to bias the photoconductive switches. (*b*) Schematic diagram of a PGL formed on a polyimide substrate, wrapped around a thin walled capillary with an outside diameter, *OD*. (*c*) A schematic illustration of the PGL reflection system. The LT-GaAs generation (*G*) and detection (*D*) photoconductive switches (shaded region) are illuminated by pump and probe laser beams (red lines).

III. Fabrication And Experimental Procedures

Devices were fabricated on a 13-µm-thick polyimide film (Kapton). PCSs were formed from an epitaxially-transferred 350-nm-thick layer of LT-GaAs [18]. The latter was obtained by molecular beam epitaxial (MBE) growth at 200 ºC on top of a 100-nm-thick AlAs sacrificial layer, itself grown on a GaAs substrate. A 15-minute-long *ex-situ* anneal at 575 ºC of the MBE-grown wafer was performed to improve the THz pulse characteristics [19]. Apiezon wax was melted onto the LT-GaAs, to act both as a structural support and as a mask for subsequent wet-etch steps. The LT-GaAs was released from the GaAs substrate by selectively etching the AlAs layer (10 % HF by volume). Using the wax support, the LT-GaAs was transferred onto the polyimide film, and left for one week to allow the LT-GaAs to bond to the surface. The wax was then removed in trichloroethylene, and the bonding process completed by baking in a vacuum oven (250 ºC, 30 mBar, 15 hrs). A single 70 µm × 70 µm square was then etched from the transferred LT-GaAs using H_2SO_4:H_2O_2:H_2O (1:8:950 by volume) to define the PCS with a sloping side-wall profile, which ensured continuity of the subsequent overlaid metal used to define both the PGL and the electrical bias arms (G and D in Fig. 1b). The PGL had a conductor width of 30 µm, and was 5 mm long from the

PCS to the open-circuit termination to separate temporally the input and reflection pulses, allowing easy discrimination for subsequent analysis. The grounded PGL connection and bias arms were defined with > 20-mm-long parasitic regions to remove interfering reflections.

The capillary was fabricated from a quartz mark-tube, with a wall thickness of 10 µm, and a 3-mm-outer diameter (Hilgenburg GmbH). Both ends of the mark-tube were removed to form a capillary, to which fluidic pipes were attached using Luer-lock connectors. Exploiting the flexibility of the thin polyimide substrate, the PGL was wrapped around the capillary, and held in place using a low-viscosity adhesive (UHU ultra fast superglue) underneath the PGL length to ensure contact was maintained over the full interaction length. The thickness of this adhesive layer was ~ 27 µm. Both the capillary and the polyimide were then mounted on a printed circuit board, and electrical interconnects made to the printed circuit board using gold bond wires.

For measurements, pulses from a Ti:sapphire laser (100 fs duration, 790 nm centre wavelength, 80 MHz repetition rate and 10 mW average power) were focused onto a 20 V biased PCS (switch *G* in Fig. 1b). The generated pulse then propagated along each of the conductors (in the bias arms, as a parasitic signal, and along the PGL sensing region). The pulse propagating along the sensing region was reflected from the end of the PGL and back towards switch *D* (Fig. 1b) where it was detected by a second, time-delayed probe laser pulse (10 mW average power). The probe pulse was optically chopped (1575 Hz), allowing lock-in detection of the resulting time-domain THz pulsed signal.

The capillary was cleaned and rinsed using the targeted analyte prior to each measurement using a flow rate of 500 µl/min for 3 minutes, determined by an automated syringe pump.

IV. RESULTS

To characterise the sensitivity of the system, measurements were taken of air (termed 'reference scan' below), water and 100 % solutions of a homologous series of primary alcohols: methanol, ethanol, propan-1-ol, butan-1-ol, hexan-1-ol and octan-1-ol. Fig. 2 shows the resulting time-domain traces both with the 'input' generated pulses (0 ps), and the 'reflected' pulses (40 to 55 ps), the latter having propagated along before being reflected from the end of the 5-mm-long PGL sensing region.

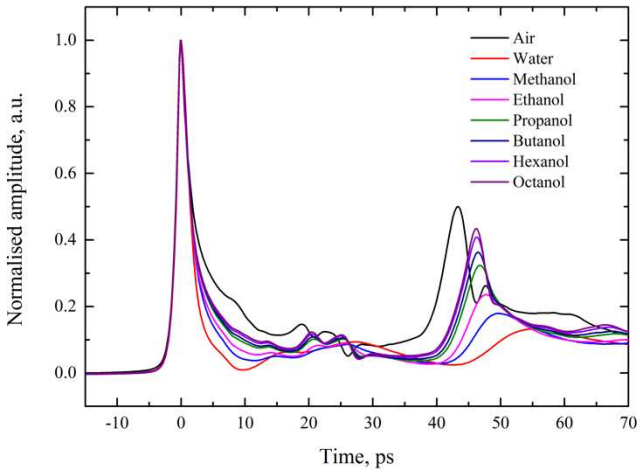

Fig. 2 Normalized TD data of air, water and a homologous series of primary alcohols, showing both the generated input pulse (0 ps) and the reflected pulse (40 – 55 ps) as the liquid filling the capillary is changed.

It is clear from Fig. 2 that both the input and reflected pulses are altered by the presence of the underlying liquid, which can be attributed to their relative dielectric properties [20, 21]. We found that for a fixed bias voltage and laser power, the amplitude of the tail of the input pulse increased with alcohol carbon chain length, while the FWHM of the pulse remained almost constant (at ~2.4 ps ± 0.2). Whilst the exact cause of the change to the input pulse is unclear, it is possible that the thermal conductance of the underlying liquid (methanol = 0.198 W/mK; ethanol = 0.161 W/mK; propanol = 0.149 W/mK; butanol = 0.147 W/mK; hexanol = 0.143 W/mK [22]), slightly affects heat dissipation, and hence the relaxation times of the charge-carriers in the LT-GaAs [23].

The time-delay, dispersion and shape of the output pulses are all affected by the presence of the underlying liquids. Fig. 3 shows the relative amplitude of the reflected pulse with respect to the input pulse, alongside the relative time delay between the input and reflected pulses, as a function of the carbon chain length of each alcohol. It can be seen that as the carbon chain length increases, the relative amplitude of the reflection increases, whilst the time delay decreases. This is in agreement with previous, free-space THz measurements of this alcohol series, which demonstrated that permittivity is inversely proportional to carbon chain length [20].

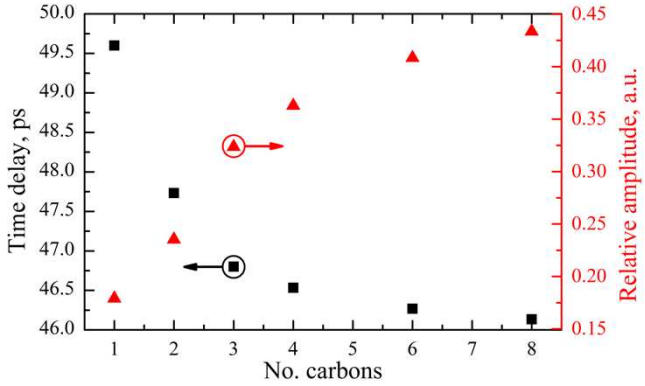

Fig. 3 Plot showing the time delay between the generated and reflected pulse maxima (black squares) and the relative amplitude of the reflected pulse with

respect to the generated pulse (red triangles). All data are plotted against the carbon chain length of the primary alcohol.

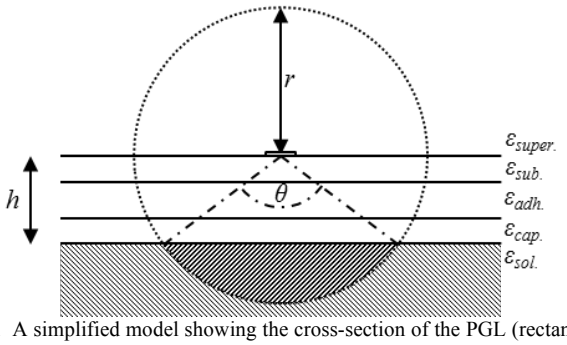

Fig. 4. A simplified model showing the cross-section of the PGL (rectangle at the center) with the extent of evanescent field (dotted circle of radius *r*) and PGL-liquid separation (*h*) highlighted. The measured permittivity of the solution (lighter shading) is found in the heavily shaded segment of the circle.

In free space measurements, the time-of-flight (TOF) refractive index can be estimated from the time-delay between a reference and sample pulse [24]. To estimate the refractive index (and in turn the relative permittivity of the solution with respect to the reference medium – air in this case) using the PGL device, we employ a simple geometric model of the substrate and sample with respect to the THz evanescent field (Fig. 4) deriving a formula for the permittivity based on our prior treatment of a similar system in Ref [6]. This model serves as a useful approximation, as a full analytical description of the field for a PGL would be rather complex. The model assumes both a uniform distribution of electric field strength around the PGL, and a circular field pattern with a frequency-independent extent of field (*r*). The permittivity of the adhesive in the potential frequency range of this system is unknown. However, using a reference–sample TOF comparison, the permittivities of the system components (polyimide, quartz and adhesive) are not required for the determination of the permittivity of the solution ($\varepsilon_{sol.}$) with respect to a reference (ε_{ref}):

$$\boldsymbol{\varepsilon_{sol.}} = \left[\frac{\boldsymbol{2\pi}}{\boldsymbol{\theta - sin\theta}}\left[\frac{\boldsymbol{c}}{\boldsymbol{d}}\left(\boldsymbol{t_{sol.} - t_{ref}}\right)\right] + \sqrt{\boldsymbol{\varepsilon_{ref}}}\right]^{\boldsymbol{2}}$$

where *d* is the propagation length (10 mm), $c = 3 \times 10^8$ ms^{-1}, and θ is related to the field extent of field (*r*) and the PGL–solution separation (*h*);

$$\boldsymbol{\theta = 2cos^{-1}\left(\frac{h}{r}\right)}$$

The time delay between the input and reflected pulse for both reference-filled and analyte-filled capillary corresponds to the reference (t_{ref}) and sample ($t_{sol.}$) signals, respectively, and provides a simple method to estimate the permittivity of the liquid from the TOF.

To confirm the dependence of permittivity on chain-length, and to validate the PGL-capillary measurements, the same chemicals were next measured on a dry-air-purged free-space THz-TDS system. Pulses from a Ti:sapphire laser (100 fs duration, 790 nm centre wavelength, 80 MHz repetition rate and 600 mW average power) were focused onto an electrically modulated (10 kHz for lock-in detection), 120 V AC biased bowtie PC emitter (2-µm-thick LT-GaAs on 500-µm-thick semi-insulating GaAs, with a 200-µm-wide gap). Using off-axis parabolic mirrors, the transmitted THz pulse was collected and focused through a liquid cell (Harrick Scientific Products Inc.) into which the liquid sample was held between two 2-mm-thick z-cut quartz windows. The transmitted THz radiation was collected and focused onto a 2-mm-thick ZnTe crystal with a collinearly coupled optical probe beam (60 mW average power) for electro-optic detection.

The separation between the quartz windows of the liquid cell, and in turn the interaction length between the THz pulses and liquid samples was changed from 100 µm, to 500 µm and 950 µm, using polytetrafluoroethylene spacers, with the results obtained showing an increase in both attenuation and propagation time as carbon chain length increased. Furthermore, for each interaction length, a distinctive change in the arrival time of the transmitted pulses for each of the primary alcohols was observed (Fig. 5). It should be noted that for water filled liquid cells with a THz interaction length of 950 µm, the transmitted pulse could not be distinguished from the noise of the system.

The resulting TD traces were analytically converted from the bipolar far-field pulse into a comparable on-chip THz-TD near-field pulse by integration to find the pulse maxima which can then be compared between the two systems. The time difference between the air-filled reference and the analyte-filled measurement was used to calculate the TOF permittivity of the solutions (ε_{sol}, see Fig. 6: triangles);

$$\boldsymbol{\varepsilon_{sol.}} = \left[\frac{\boldsymbol{c}}{\boldsymbol{d}}\left(\boldsymbol{t_{sol.} - t_{ref}}\right) + \sqrt{\boldsymbol{\varepsilon_{ref}}}\right]^{\boldsymbol{2}}$$

where *d* is the THz path length through the liquid cell.

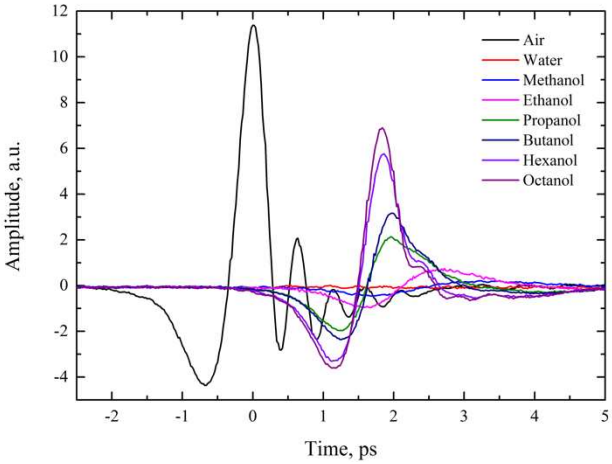

Fig. 5 Free-space THz TDS data for air, water and the homologous series of primary alcohols held in a liquid cell with a window separation of 950 µm.

The TOF permittivity of the solutions using the on-chip THz-TD system was found using an air-filled capillary as a reference measurement ($\varepsilon_{ref} = 1$; $t_{ref} = 43.2$ ps; $r = 100$ µm

[6]; h = 50 μm). The results show the reduction in permittivity of primary alcohols with increasing carbon chain length (see Fig. 6; black circles).

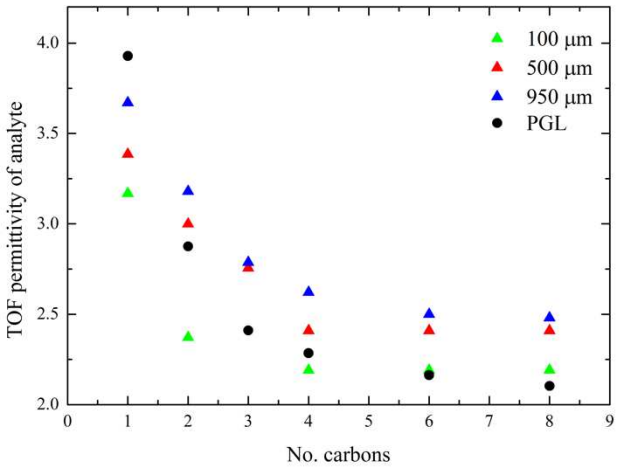

Fig. 6 Calculation of TOF permittivity for PGL devices (circles) and free-space (triangles) using the time delay data taken from Fig. 3 and 5.

Upon inspection, it is clear that the TOF permittivity is dependent on interaction length, suggesting a bandwidth dependence of the pulse propagation velocities. The TOF permittivity recorded should arise approximately from an averaged integration of the frequency components of the permittivity with respect to the bandwidth of the transmitted pulse. Therefore, to correlate the free-space and PGL data, the length of interaction between the liquid and THz pulse, and therefore the frequency bandwidth of the THz pulse, need to be refined by altering the sample thickness. Furthermore, the frequency spectra of the incident pulses are different between the two systems, with the PGL system supporting lower frequency elements whereas the free-space THz-TDS system has a larger bandwidth. Nevertheless, the free-space THz-TDS demonstrates a comparable change in permittivity with the primary alcohol's carbon chain length.

Using the measured TOF permittivities (Fig. 6) and the relative amplitude of the reflected signal (Fig. 3), R_A, the change in attenuation coefficient, Δα, can be calculated by [25, 26];

$$\boldsymbol{\Delta\alpha = \ln\left(\frac{4\sqrt{\varepsilon_{sol.}}}{R_A\left(\sqrt{\varepsilon_{sol.}}+1\right)^2}\right)}$$

Due to the lack of frequency information, no absolute value for the attenuation can be recorded, however the resulting decay in attenuation (relative to that for methanol) with increasing carbon chain length (Fig. 7) agrees with the behaviour of frequency-dependent free-space measurements taken elsewhere [27], as well as agreeing with the observed change in the reflected pulse shape (Fig. 2).

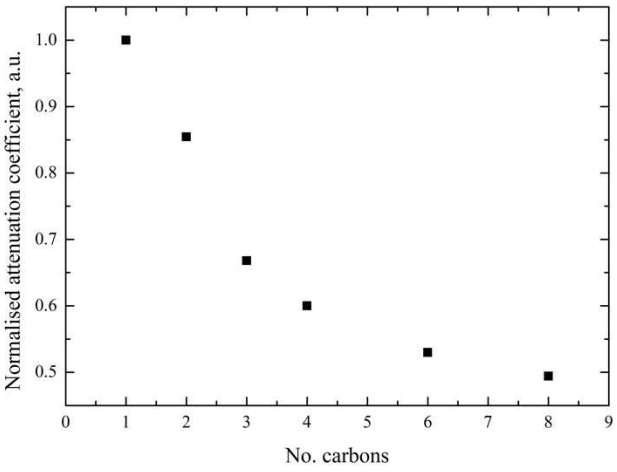

Fig. 7 Normalized attenuation coefficients of the homologous series of primary alcohol calculated using data taken from Fig. 3 .

V. Conclusion

We have developed a THz-TD liquid sensing system using flexible polyimide films with an integrated THz waveguide. PGLs were wrapped around a thin-walled, liquid-filled quartz capillary allowing the analysis of liquids enclosed therein. The design offers minimal restrictions on the liquid, requiring only chemical compatibility with the quartz capillaries used (although use of other capillary materials is possible). Furthermore, due to the in-built reference, the numerical values for material properties (in particular, the electrical permittivity) are not necessary for calculating the relative permittivity of the enclosed liquids.

When compared to a free-space THz-TDS system, utilising a liquid cell, the PGL-capillary system showed a similar shift in TOF permittivity for a homologous series of primary alcohols, but with an improved signal-to-noise ratio, and significantly greater interaction length.

We note that whilst the TOF method presented here provides only a relative approximation of the permittivity of the enclosed samples, a transmission based waveguide mesaurment could in principle be utilised to recover the bandwidth of the resulting spectra in the frequency domain by reducing the interaction length, to obtain a more accurate representation of the permittivities of fluidic samples. This would further strengthen comparison with the free-space THz-TDS data, in addition to permitting more definitive values for permittivity and attenuation to be extracted.

References

[1] U. Heugen, G. Schwaab, E. Bründermann, M. Heyden, X. Yu, D. M. Leitner, *et al.*, "Solute-induced retardation of water dynamics probed directly by terahertz spectroscopy," *Proceedings of the National Academy of Sciences,* vol. 103, pp. 12301-12306, 2006.

[2] A. J. Baragwanath, G. P. Swift, D. Dai, A. J. Gallant, and J. M. Chamberlain, "Silicon based microfluidic

cell for terahertz frequencies," *Journal of Applied Physics,* vol. 108, p. 013102, 2010.

[3] H. Hirori, K. Yamashita, M. Nagai, and K. Tanaka, "Attenuated Total Reflection Spectroscopy in Time Domain Using Terahertz Coherent Pulses," *Japanese Journal of Applied Physics,* vol. 43, p. L1287, 2004.

[4] P. U. Jepsen, J. K. Jensen, and U. Møller, "Characterization of aqueous alcohol solutions in bottles with THz reflection spectroscopy," *Optics Express,* vol. 16, pp. 9318-9331, 2008.

[5] Y. C. Shen, P. C. Upadhya, H. E. Beere, E. H. Linfield, A. G. Davies, I. S. Gregory*, et al.*, "Generation and detection of ultrabroadband terahertz radiation using photoconductive emitters and receivers," *Applied Physics Letters,* vol. 85, pp. 164-166, 2004.

[6] C. Russell, C. D. Wood, A. D. Burnett, L. Li, E. H. Linfield, A. G. Davies*, et al.*, "Spectroscopy of polycrystalline materials using thinned-substrate planar Goubau line at cryogenic temperatures," *Lab on a Chip,* vol. 13, pp. 4065-4070, 2013.

[7] T. Ohkubo, M. Onuma, J. Kitagawa, and Y. Kadoya, "Micro-strip-line-based sensing chips for characterization of polar liquids in terahertz regime," *Applied Physics Letters,* vol. 88, p. 212511, 2006.

[8] S. Laurette, A. Treizebre, F. Affouard, and B. Bocquet, "Subterahertz characterization of ethanol hydration layers by microfluidic system," *Applied Physics Letters,* vol. 97, p. 111904, 2010.

[9] S. Laurette, A. Treizebre, and B. Bocquet, "Co-integrated microfluidic and THz functions for biochip devices," *Journal of Micromechanics and Microengineering,* vol. 21, p. 065029, 2011.

[10] A. Raj, W. S. Holmes, and S. R. Judah, "Wide bandwidth measurement of complex permittivity of liquids using coplanar lines," *Instrumentation and Measurement, IEEE Transactions on,* vol. 50, pp. 905-909, 2001.

[11] S. Yanagi, M. Onuma, J. Kitagawa, and Y. Kadoya, "Propagation of Terahertz Pulses on Coplanar Strip-lines on Low Permittivity Substrates and a Spectroscopy Application," *Applied Physics Express,* vol. 1, p. 012009, 2008.

[12] M. Y. Frankel, S. Gupta, J. Valdmanis, and G. A. Mourou, "Terahertz attenuation and dispersion characteristics of coplanar transmission lines," *Microwave Theory and Techniques, IEEE Transactions on,* vol. 39, pp. 910-916, 1991.

[13] D. Gacemi, A. Degiron, M. Baillergeau, and J. Mangeney, "Identification of several propagation regimes for terahertz surface waves guided by planar Goubau lines," *Applied Physics Letters,* vol. 103, p. 191117, 2013.

[14] S. Laurette, A. Treizebre, A. Elagli, B. Hatirnaz, R. Froidevaux, F. Affouard*, et al.*, "Highly sensitive terahertz spectroscopy in microsystem," *RSC Advances,* vol. 2, pp. 10064-10071, 2012.

[15] D. J. Beebe, G. A. Mensing, and G. M. Walker, "PHYSICS AND APPLICATIONS OF MICROFLUIDICS IN BIOLOGY," *Annual Review of Biomedical Engineering,* vol. 4, pp. 261-286, 2002.

[16] J. N. Lee, C. Park, and G. M. Whitesides, "Solvent Compatibility of Poly(dimethylsiloxane)-Based Microfluidic Devices," *Analytical Chemistry,* vol. 75, pp. 6544-6554, 2003.

[17] V. Miseikis, "The Interaction of Graphene with High-Frequency Acoustic and Electromagnetic Waves," *PhD Thesis, University of Leeds,* p. 141, 2012.

[18] E. Yablonovitch, D. M. Hwang, T. J. Gmitter, L. T. Florez, and J. P. Harbison, "Van der Waals bonding of GaAs epitaxial liftoff films onto arbitrary substrates," *Applied Physics Letters,* vol. 56, pp. 2419-2421, 1990.

[19] I. S. Gregory, C. Baker, W. R. Tribe, M. J. Evans, H. E. Beere, E. H. Linfield*, et al.*, "High resistivity annealed low-temperature GaAs with 100 fs lifetimes," *Applied Physics Letters,* vol. 83, pp. 4199-4201, 2003.

[20] Y. Yomogida, Y. Sato, R. Nozaki, T. Mishina, and J. i. Nakahara, "Dielectric study of normal alcohols with THz time-domain spectroscopy," *Journal of Molecular Liquids,* vol. 154, pp. 31-35, 2010.

[21] C. Rønne, L. Thrane, P.-O. Åstrand, A. Wallqvist, K. V. Mikkelsen, and S. R. Keiding, "Investigation of the temperature dependence of dielectric relaxation in liquid water by THz reflection spectroscopy and molecular dynamics simulation," *The Journal of Chemical Physics,* vol. 107, pp. 5319-5331, 1997.

[22] M. J. Assael, E. Charitidou, and C. A. Nieto de Castro, "Absolute measurements of the thermal conductivity of alcohols by the transient hot-wire technique," *International Journal of Thermophysics,* vol. 9, pp. 813-824, 1988.

[23] A. G. Markelz and E. J. Heilweil, "Temperature-dependent terahertz output from semi-insulating GaAs photoconductive switches," *Applied Physics Letters,* vol. 72, pp. 2229-2231, 1998.

[24] D. M. Mittleman, S. Hunsche, L. Boivin, and M. C. Nuss, "T-ray tomography," *Optics Letters,* vol. 22, pp. 904-906, 1997.

[25] J. Chen, Y. Chen, H. Zhao, G. J. Bastiaans, and X. C. Zhang, "Absorption coefficients of selected explosives and related compounds in the range of 0.1-2.8 THz," *Optics Express,* vol. 15, pp. 12060-12067, 2007.

[26] M. Scheller and M. Koch, "Fast and Accurate Thickness Determination of Unknown Materials using Terahertz Time Domain Spectroscopy," *Journal of Infrared, Millimeter, and Terahertz Waves,* vol. 30, pp. 762-769, 2009.

[27] M. S. Zafar, F. I. Zafar, A. Shamim, and Z. Arif, "Measurements of refractive indices and power absorption coefficients of liquids at 2.54 THz (118 μm)," *Infrared Physics,* vol. 24, pp. 505-509, 1984.

Christopher Russell received his BEng in Electronic and Electrical Engineering from the University of Leeds before completing a PhD in on-chip THz-TDS systems at the Institute of Microwaves and Photonics within the same university. Following post-doctoral studies on the same project, he has since moved onto the study of electrical contacts for the field of neuroscience.

Matthew Swithenbank received his BEng and MEng in Electronic and Electrical Engineering from the University of Leeds in 2013. He is currently a PhD student in the Institute of Microwaves and Photonics at the University of Leeds, where his research concerns terahertz spectroscopy in microfluidic systems.

Christopher D. Wood obtained a BSc in Physics with Electronics from the University of Leeds, followed by an MSc (dist) in Nanoscale Science and Technology with the University of Sheffield. He returned to Leeds to pursue a PhD in On-chip Terahertz Technology, where he is now currently employed as a tenure-track University Research Fellow in High-frequency and Mesoscopic Electronics.

Andrew D. Burnett received his MChem in Chemistry from the University of Bradford in 2004 before pursuing is Ph.D. in THz spectroscopy at the University of Leeds completing his studies in 2008. Since then Andrew has continued to work at Leeds while holding an EPSRC Postdoctoral Fellowship. He is currently a Teaching and Research Fellow in Physical Chemistry and Terahertz Technology.

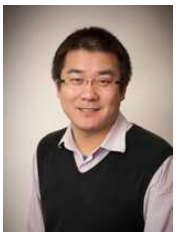

Lianhe Li received the Ph.D. degree in microelectronics and solid-state electronics from the Institute of Semiconductors, Chinese Academy of Sciences, Beijing, China, in 2001. From 2001 to 2003, he was with the Laboratoire de Photonique et des Nanostructures, Centre National de la Recherche Scientifique (CNRS), France, where he was engaged in molecular beam epitaxy (MBE) growth and characterization of low-bandgap GaAs-based III-V diluted nitride materials and devices with a particular emphasis on 1300–1550 nm telecom wavelength applications. In July 2003, he joined EPFL, Lausanne, Switzerland, as a Scientific Collaborator, where he was working on InAs quantum dots for lasers and superluminescent LEDs and single quantum dot devices. He is currently with the School of Electronic and Electrical Engineering, University of Leeds, U.K.

Edmund Harold Linfield received the B.A. (Hons.) degree in physics from the University of Cambridge, Cambridge, U.K., in 1986 and the Ph.D. degree from the University of Cambridge in 1991. He continued his research at the Cavendish Laboratory, University of Cambridge, becoming an Assistant Director of Research and a Fellow of Gonville and Caius College, Cambridge in 1997. In 2004, he joined the University of Leeds to take up the Chair of Terahertz Electronics, where he is currently also the Director of Research in the School of Electronic and Electrical Engineering. His research interests include semiconductor growth and device fabrication, terahertz-frequency optics and electronics, and nanotechnology. He shared the Faraday Medal and Prize from the Institute of Physics in 2014, and received a Wolfson Research Merit award from the Royal Society in 2015.

Alexander Giles Davies received the B.Sc. (Hons.) degree in Chemical Physics from the University of Bristol, UK, in 1987, and the Ph.D. degree from the University of Cambridge, UK, in 1991.

In 1991, he joined the University of New South Wales, Sydney, Australia, supported by an Australian Research Council Fellowship, before returning to the Cavendish Laboratory, University of Cambridge in 1995 as a Royal Society University Research Fellow. Since 2002 he has been with the School of Electronic and Electrical Engineering, University of Leeds, as Professor of Electronic and Photonic Engineering, and is currently also Pro-Dean for Research and Innovation in the Faculty of Engineering. His research interests include the optical and electronic properties of semiconductor devices, terahertz frequency electronics and photonics, and the exploitation of biological properties for nanostructure engineering.

Professor Davies is a Fellow of the Institute of Physics, and both a Chartered Physicist and Engineer. He received a Wolfson Research Merit award from the Royal Society in 2011, and shared the Faraday Medal and Prize from the Institute of Physics in 2014.

John E. Cunningham received his BSc in Physical Sciences from University College London in 1995, MSc from Imperial in 1996, and PhD from the University of Cambridge in 2000. He is now Professor of Nanoelectronics at the University of Leeds, with research interests in mesoscopic systems, surface acoustic waves, and terahertz electronics and photonics.